A vacuum ultraviolet photoionization time-of-flight mass spectrometer with high sensitivity for study of gas phase radical reaction in flow tube

Zuoying Wen[a,b], Xiaofeng Tang[a*], Chengcheng Wang[a,b], Christa Fittschen[c], Tao Wang[a], Cuihong Zhang[a,b], Jiuzhong Yang[d], Yang Pan[d], Fuyi Liu[d], Weijun Zhang[a,e*]

[a] Laboratory of Atmospheric Physico-Chemistry, Anhui Institute of Optics and Fine Mechanics, Chinese Academy of Sciences, Hefei, 230031 Anhui, China.

[b] Graduate School, University of Science and Technology of China, Hefei, 230026 Anhui, China.

[c] University Lille, PC2A, UMR CNRS-ULille 8522, Cite Scientifique Bat. C11, F-59655 Villeneuve d'Ascq, France.

[d] National Synchrotron Radiation Laboratory, University of Science and Technology of China, Hefei, 230029 Anhui, China.

[e] School of Environmental Science and Optoelectronic Technology, University of Science and Technology of China, Hefei, 230026 Anhui, China.

Abstract: Photoionization mass spectrometry (PIMS) as a powerful analytical method has been widely utilized and provided valuable insight in the field of gas-phase reactions. Here, a highly sensitive vacuum ultraviolet (VUV) photoionization time-of-flight mass spectrometer combined with a microwave discharge generator and a fast flow tube reactor has been developed to study radical reactions of atmospheric and combustion interests. Two kinds of continuous light sources, the tunable VUV synchrotron radiation at Hefei, China for isomer-specific product detection and a commercial krypton discharge lamp for time-consuming kinetic measurements, are employed as photoionization sources in the apparatus. A multiplexed detection with high sensitivity (the limit of detection, LOD ~ 0.8 ppb) and high mass resolution ($M/\Delta M$ ~ 2100) has been approached. As representative examples, the self-reaction of the methyl radical, CH_3, and the reaction of the methyl radical with molecular oxygen are studied and multiple species including reactive radicals and isomeric/isobaric products are detected and identified. In addition, some preliminary results related to the reaction kinetics are also presented.

Keywords: Photoionization mass spectrometer, radical reaction, kinetics, flow tube, methyl radical, methyl peroxy radical.

Corresponding authors: * tangxf@aiofm.ac.cn (X. Tang); wjzhang@aiofm.ac.cn (W. Zhang)

1. Introduction

Radical reactions play an essential role in atmospheric and combustion chemistry and have been a subject of great interest in the past few decades. Understanding of their underlying mechanisms, usually involving multi-channel processes, relies on the determination of reaction rate constants and chemical compounds involved in the reactions, including both stable and reactive transient species.[1-4] Thus the direct measurement of the abundance and structure information of these key species with sufficient time resolution is needed. In the past, significant advances have been made in revealing complex mechanism by applying a great deal of analytical methods such as absorption spectroscopy[5], laser-induced fluorescence (LIF)[6], cavity ring-down spectroscopy (CRDS)[7,8], chemical ionization mass spectrometry (CIMS)[9,10] and photoionization mass spectrometry (PIMS)[11-13] combined with various flow reactor or flash photolysis setups[14,15].

Among the above possible analytical methods, PIMS[2,3,16], especially combined with molecular beam sampling and tunable vacuum ultraviolet (VUV) synchrotron light sources, can detect almost all the reactants and products simultaneously and has provided valuable insight in combustion and other fields. In particular, photoionization efficiency spectra (PIES) corresponding to each mass are measured by scanning synchrotron photon energy and then their individual ionization energies (IEs) and structure-specific information can be obtained.[17-19] Recently, photoelectron photoion coincidence spectroscopy (PEPICO), analyzing both the photoion and the photoelectron from photoionization in coincidence, has been utilized at several synchrotron facilities to investigate radical reactions.[20-23] The mass-selected threshold photoelectron spectra (TPES) with high energy resolution obtained from PEPICO offer greater selectivity than PIMS.[24,25]

The capabilities of synchrotron-based PIMS and PEPICO as universal, multiplexed, selective and sensitive analytical methods have already been demonstrated. However, in comparison to the above laser-based spectroscopy methods that are usually applied to analyze small molecules with concentrations down to ppb/ppt levels,[7,8] the sensitivities of the synchrotron-based PIMS and PEPICO are still limited. The limit of detection (LOD) of the PIMS endstation for combustion research at Hefei synchrotron was reported to be

at the level of sub-ppm.[26,27] A molecular density of N = 8.3 x 10^{10} cm^{-3} at 4 Torr total pressure, corresponding to a mole fraction of 6.5 x 10^{-7} (~ 0.65 ppm), was obtained with the time-resolved multiplexed photoionization mass spectrometer (MPIMS) at the Advanced Light Source.[13] No information on the sensitivity of the PEPICO setups[28-31] could be found in the literature. But, restricted by the false coincidence background, the sensitivity of PEPICO should be less than that of PIMS and still remained to be improved, especially for applications in the atmosphere-related research using generally low concentrations.

In this article, we present a custom-made highly sensitive VUV photoionization orthogonal time-of-flight (TOF) mass spectrometer with LOD of ~ 0.8 ppb and high mass resolution ($M/\Delta M$ ~ 2100) to study radical reactions of atmospheric and combustion interests. A fast flow tube consisting of a main pyrex tube and a coaxial movable injector is installed as reactor in which the reactions are initiated using a microwave discharge generator. A continuous molecular beam is formed for sampling and both stable and reactive transient species involved in the reaction can be detected. Depending on the problems to be resolved, two kinds of VUV light sources, the continuously tunable VUV synchrotron radiation at Hefei, China,[27,28] for isomer-specific product detection and a commercial krypton discharge lamp for time-consuming kinetic measurements, have been employed as photoionization sources in the apparatus. The combination of the continuous molecular beam sampling and the continuous VUV photoionization light sources is beneficial to optimize the sensitivity of the species detection. As representative examples, the self-reaction of the methyl radical, CH_3, and the bi-molecular reaction of the methyl radical and molecular oxygen have been chosen to characterize the apparatus.

2. Experimental setup

The experimental setup developed in the laboratory consists of three main components: a fast flow tube reactor, VUV photoionization light sources and a photoionization orthogonal reflectron TOF mass spectrometer. A schematic diagram is presented in Figure 1, together with the photographs of the microwave discharge and the molecular beam sampling interface.

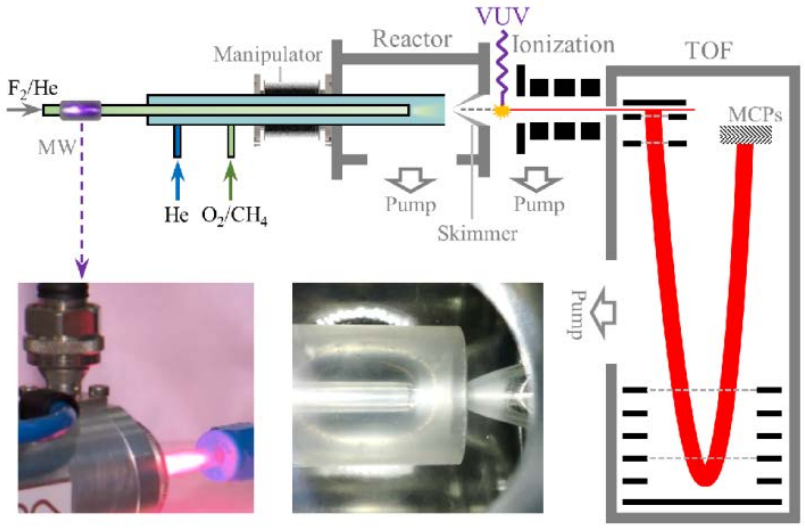

Figure 1. Schematic diagram of the experimental setup, mainly consisting of a fast flow tube reactor, VUV photoionization light sources and an orthogonal reflectron TOF mass spectrometer. The two inserting photographs show the microwave discharge and the molecular beam sampling interface. The ion trajectories in the mass spectrometer are exemplified and marked in red.

2.1 Fast flow tube reactor

The fast flow tube reactor is composed of a 75 cm long pyrex main tube with 30 mm outer diameter, 26 mm inner diameter, and a 100 cm long coaxial movable injector with 6 mm outer diameter, 4 mm inner diameter. The inner surface of the main tube and the inner and outer surfaces of the injector are coated with halocarbon wax to minimize radical loss on the walls. The main tube is also built with several arms allowing direct injection of various gaseous reactants. The component gases are measured with individual calibrated mass flow controllers (D07-7B, Sevenstar, China). The pressure in the middle of the flow tube reactor is metered using a capacitance manometer (CDG-500, Agilent) and maintained at 1 - 10 Torr by a closed-loop feedback throttle valve installed between the reactor chamber and the vacuum pump.

Presently fluorine atoms as radical initiator are produced by a microwave discharge generator (2450 MHz, GMS-200W, Sairem, France) in a mixture of 1% F_2 diluted in He gas and introduced into the flow tube reactor through either a side arm of the main tube or the injector. The F_2 dissociation efficiency is measured with its ion signal change in the synchrotron photoionization mass spectra and its value can be approached to ~ 95% with a microwave discharge power of P = 100 W. Other reactant gases like CH_4 and O_2 and the He carrier gas are fed into the reactor in large excess with respect to the fluorine atom

concentration.

The total gas flow is about 1 Standard Liter per Minute (SLM) and typical flow velocities range from 3 to 24 m/s. The Reynolds number, Re, used to distinguish between laminar and turbulent flows, is defined as[32]

$$Re = \rho v d / \mu \qquad (1)$$

where d is the inner diameter of the flow tube, ρ, v and μ are the density, the velocity and the dynamic viscosity of the fluid. Here the Reynolds number is calculated to be ~ 7, indicating that the flow fluid is laminar and thus the plug-flow approximation is valid in the fast flow tube reactor.[12]

In the fast flow tube, the distance between the tip of the injector and the detection region, L, is adjusted and then the reaction time, t, can be calculated with the flow velocity through the relation below.

$$t = L / v \qquad (2)$$

Kinetics experiments can be performed by measuring the ion signals in the photoionization mass spectra at various reaction times with different reactant concentrations.

As shown in Figure 1, the fast flow tube reactor is mounted on a manually controlled XYZ manipulator inside the reactor chamber of the photoionization mass spectrometer and its position is tuned in real-time to optimize the ion signal. Downstream of the fast flow tube reactor, a 1-mm-diameter quartz skimmer is installed for sampling and connects the reactor chamber and the ionization chamber of the photoionization mass spectrometer. After passing through the flow tube reactor, the gaseous mixtures are sampled through the skimmer and are expanded into the ionization chamber. A continuous molecular beam is formed and both the stable and the reactive transient species involved in the radical reactions can be sampled and detected.

2.2 VUV photoionization light sources

In the ionization chamber of the mass spectrometer the continuous molecular beam crosses the beam of the VUV photoionization light source with a right angle in the photoionization region. Depending on the problems to be resolved, two kinds of photoionization light sources have been used in the apparatus: (i) the continuously tunable VUV synchrotron light from the Combustion and Flame Beamline of National

Synchrotron Radiation Laboratory (NSRL) in Hefei, China,[27] for isomer-specific detection and (ii) a commercial krypton discharge lamp (PKS 106, Heraeus) with two fixed atomic resonance lines, hν = 10.0 and 10.6 eV for time-consuming kinetic measurements. The Hefei synchrotron light is with a repetition rate of 204 MHz quasi-continuously operated. The combination of the continuous or quasi-continuous VUV photoionization light source and the continuous molecular beam sampling is beneficial to increase the sensitivity of the species detection.

These two VUV photoionization light sources have their own characters and are complementary in experiments. The VUV synchrotron radiation has a wide energy range with high brightness and its wavelength can be continuously and quickly changed. PIES corresponding to each mass are acquired by scanning synchrotron photon energy and then their IEs can be measured and used to obtain information on the structure of the molecule corresponding to the mass peaks and to discriminate different isomers. But the synchrotron beamtime is very limited and only available to us for a short time every year. The other light source, the krypton discharge lamp, is compact with a low cost and can be used in the laboratory for infinite time, and is thus especially suitable for kinetics measurements which often need a lot of measurement time. Some other discharge lamps filled with different gases are also available in our laboratory. The limitation of the discharge lamp is that its wavelength is not tunable and only several discrete atomic lines can be used, even with different discharge lamps. The krypton discharge lamp is sealed with a MgF_2 window and its photon flux is estimated to be ~ 10^{12} photons/s. In the apparatus, the krypton discharge lamp is directly installed inside the ionization chamber and very close to the photoionization region to enhance the detection sensitivity.

On the synchrotron beamline, photons emitted from an undulator are dispersed by a monochromator equipped with two gratings, 200 and 400 l/mm, covering the photon energy ranges of 5 - 13 eV and 11 - 21 eV, respectively.[27] A gas filter located just before the apparatus is filled with noble gas (presently Ar for hν < 15.5 eV) to eliminate the high-order harmonic radiations from the undulator. With the resonant absorption lines of Ar in the gas filter, the absolute photon energy of the beamline is calibrated on-line within an accuracy of ± 5 meV. The photon flux of the beamline with the current of 300 mA in the electron storage ring is measured to be ~ 10^{13} photons/s. A photodiode (SXUV-

100, IRD Inc.) with an electrometer (6517A, Keithley) installed behind the photoionization region is adopted to record the photon flux and then to normalize the ion signals in the photon energy scans.

2.3 Photoionization orthogonal reflectron time-of-flight mass spectrometer

The photoionization mass spectrometer is custom-made with a configuration of orthogonal injection reflectron TOF mass spectrometer,[33] as shown in Figure 1. The photoionization orthogonal reflectron TOF mass spectrometer is composed of three vacuum chambers, the reactor chamber, the ionization chamber and the TOF chamber, and their individual pressures and vacuum pumps are listed in Table 1. The reactor chamber is evacuated by a dry scroll pump (10 l/s, XDS35i, Edwards), where the closed-loop feedback throttle valve is installed between them to maintain the pressure of the flow tube reactor. The ionization chamber is evacuated by a turbo-molecular pump (400 l/s, nEXT400D, Edwards) and the TOF chamber by two turbo-molecular pumps (300 l/s, nEXT300D, Edwards and 300 l/s, 350i, Leybold). The turbo-molecular pumps of the ionization chamber and TOF chamber are roughed by the same dry scroll pump (10 l/s, XDS35i, Edwards). The background pressure without gas load in the reactor chamber is less than 10^{-2} Torr, and in the ionization and TOF chambers it is in the low 10^{-7} Torr range.

Table 1. The working pressures and the vacuum pumps of the photoionization mass spectrometer.

Chambers	Pressures (Torr)	Pumps
Reactor chamber	1 - 10	10 l/s dry mechanic pump
Ionization chamber	~ 10^{-4}	400 l/s turbo-molecular pump
TOF chamber	~ 10^{-6}	600 l/s turbo-molecular pump

The present apparatus's design is inspired by the combustion endstation of the synchrotron beamline.[27] But in comparison to the tightly focused synchrotron photon beam, the VUV light emitted from the krypton discharge lamp has a much larger spot size in the photoionization region. So in the present design, the ion extraction optics at the ion guide part of the photoionization mass spectrometer has been redesigned. An electric penetrating field[34] is employed in the ion extraction optics to make sure that almost all of the ions produced in the ionization region (~ 3 x 3 x 8 mm^3) can be extracted and collected; details will be described in a future publication. In addition, with

the orthogonal injection configuration, the pressure inside the ionization chamber can be increased with only little influence on the TOF chamber, and therefore allowing more species to be sampled and ionized. Thus, even with the VUV discharge lamp as photoionization light source, an efficient detection with high sensitivity and low LOD still can be achieved.

After the extraction optics, an einzel lens with several cylindrical tubes is installed and used to focus and transmit the ions.[35] After crossing over a 2-mm-diameter circular hole connecting the ionization chamber and the TOF chamber, the ion beam will be pushed and accelerated by dual pulses with positive and negative voltages applying on the first and the third electrodes of the extraction region of the photoionization mass spectrometer.[27,33] The repetition rates of the pulse voltages are adjusted at 35 kHz and ions with mass up to 400 amu can be detected. After acceleration, these ions fly into the field-free and the reflectron regions with a double space focusing configuration and then back again. Finally these ions are detected by a pair of micro-channel plates (MCPs, 50 mm diameter) in a chevron configuration. The signals from the MCPs are amplified by an amplifier and recorded by a multiscaler counter (P7888-2, FAST ComTec, Germany). The PIES corresponding to each mass can be acquired by continuously scanning the synchrotron photon energy. The photoionization mass spectrometer has a compact design with a total ion flight length of ~ 1 m and its performances has been tested and will be discussed in the following section.

3. Preliminary results

In this section we will describe the overall performance of the photoionization mass spectrometer, including the mass resolution and the limit of detection, and then its first applications in the self-reaction of the methyl radical and the bi-molecular reaction of the methyl radical with molecular oxygen.

3.1 Mass resolution

A bottle of standard gaseous mixtures with calibrated concentrations of benzene (C_6H_6, 10.8 ppm), toluene (C_7H_8, 10.5 ppm) and p-xylene (C_8H_{10}, 10.2 ppm), purchased from Nanjing Special Gases CO. LTD, China, is used to calibrate the mass spectra and to test the performances of the photoionization mass spectrometer. The standard gas is fed

into the fast flow tube reactor with the pressure fixed at 2 Torr. Figure 2(a) shows the photoionization mass spectrum of the standard gas recorded with the krypton discharge lamp. Three intense and sharp peaks are clearly observed in the mass spectrum and correspond to the molecular ions of benzene (m/z = 78), toluene (m/z = 92) and p-xylene (m/z = 106), respectively. Another three accompanying peaks at m/z = 79, 93 and 107 can be identified in the mass spectrum too and are assigned to their ^{13}C isotopic species.

The IEs of benzene, toluene and p-xylene locate at 9.244,[36] 8.828[37] and 8.445 eV[38], respectively, and are close to the photon energies of the photoionization light source. The species contained in the standard gas are ionized at their thresholds and so only their molecular ion peaks without fragmentation are detected in the photoionization mass spectrum. In addition, as shown in the insert part of Figure 2(a), from the width of the peak of p-xylene in the mass spectrum, the mass resolution of the photoionization mass spectrometer is determined to be M/ΔM ~ 2100 (the full width at half maximum, FWHM).

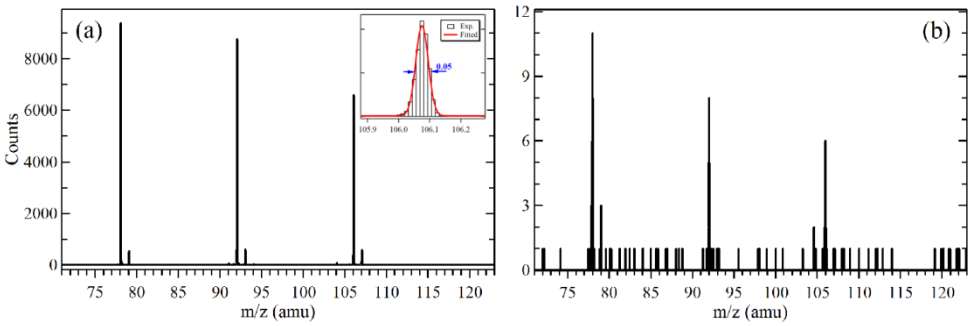

Figure 2. Photoionization time-of-flight mass spectra of the gaseous mixtures of benzene, toluene, and p-xylene recorded with their concentrations of (a) 10 ppm and (b) 20 ppb, both of which were accumulated for 100 seconds. The insert in (a) shows a zoom of the ion peak of p-xylene with a mass resolution of M/ΔM ~ 2100 (FWHM). The krypton discharge lamp is used as photoionization light source.

3.2 The limit of detection

Sensitivity is one of the key performance indices of the photoionization mass spectrometer and so it is necessary to measure it quantitatively. The sensitivity of the photoionization mass spectrometer with the fast flow tube as gas inlet is also measured with the calibrated standard gas. Helium is used as the diluted gas and added into the fast flow tube with the calibrated standard gas. The ratios of the helium gas and the calibrated standard gas are accurately adjusted with their individual calibrated mass flow controllers.

The pressure inside the fast flow tube is still fixed at 2 Torr and the krypton discharge lamp is used as the photoionization light source. Figure 3 presents a series of the ion intensities obtained in the photoionization mass spectra versus their individual concentrations. We can see that the ion intensities of benzene, toluene and p-xylene increase linearly with their concentrations.

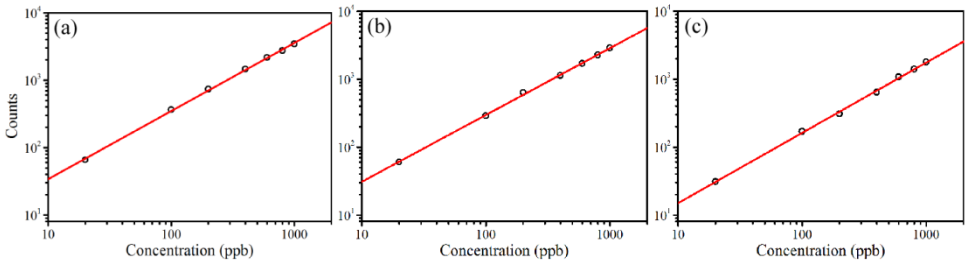

Figure 3. The ion intensities of (a) benzene, (b) toluene, and (c) p-xylene in the photoionization mass spectra as a function of their concentrations, recorded with the krypton discharge lamp as photoionization light source.

The standard gas is diluted to concentrations down to 20 ppb and the photoionization mass spectrum is recorded with the discharge lamp, shown in Figure 2(b). The photoionization mass spectrum is accumulated for 100 seconds and exhibits nearly zero background signals. The three ion peaks of benzene, toluene and p-xylene with their concentrations of 20 ppb can clearly be observed with high signal-to-noise ratios.

According to the method of Williams et al.,[39] the LOD for the photoionization mass spectrometer with the continuous molecular beam sampling can be determined from the above photoionization mass spectrum of the gaseous mixtures. The noise level is determined using the variance σ of the amplitude of the signal between mass peaks and the mean value of the noise is defined as baseline B. The LOD is then calculated for a signal-to-noise ratio of 3 according to the relation,[40]

$$LOD = 3\sigma c / (S - B) \qquad (3)$$

where S is the signal peak height of the target molecule in the photoionization mass spectrum and c is its concentration.

From the photoionization mass spectrum of Figure 2(b), the LOD of the photoionization mass spectrometer with the fast flow tube inlet is measured to be ~ 0.8 ppb, corresponding to a molecular density of $N = 4.5 \times 10^7$ cm^{-3} at a pressure of 2 Torr within the flow tube. The ion signals in the photoionization mass spectra increase with

the pressure inside the fast flow tube and a lower LOD can be acquired with a higher pressure. As we have discussed in Sec. 2, several strategies like the penetrating electric field to extract the ions, the orthogonal injection configuration to sample more species, and the combination of the continuous molecular beam and the continuous VUV light source to maximize photoionization, have already been employed in the present apparatus and contribute to its high sensitivity. The LOD of the present photoionization mass spectrometer is much lower than those of the PIMS endstation at Hefei synchrotron (LOD ~ sub ppm)[26,27] and the MPIMS setup at the Advanced Light Source (LOD ~ 0.65 ppm)[13].

3.3 The CH_3 + CH_3 self-reaction

As a representative example, the self-reaction of the methyl radical has been chosen and investigated with the photoionization mass spectrometer. In the experiments, fluorine atoms produced in the microwave discharge (MW) of F_2 diluted in He are used as radical initiator and the methyl radicals are formed in the fast flow tube via H-abstraction through the following reactions,

$$F_2 + MW \rightarrow F + F \qquad (4)$$

$$F + CH_4 \rightarrow CH_3 + HF \qquad (5)$$

where the concentration of methane is much higher than that of the fluorine atoms. In the fast flow tube the methyl radicals decay mostly through fast self-reaction and produce ethane, which has also been investigated in the past by several groups.[41,42]

$$CH_3 + CH_3 \rightarrow \text{products} \qquad (6)$$

This self-reaction is a second-order reaction and the concentration of the methyl radical, $[CH_3]$, will change with reaction time through the following relation

$$\frac{d[CH_3]}{dt} = -2k_1\,[CH_3]^2 \qquad (7)$$

$$\frac{1}{[CH_3]} = \frac{1}{[CH_3]_0} + 2k_1 t \qquad (8a)$$

where $[CH_3]_0$ is the initial concentration of CH_3, t is the reaction time and k_1 is the reaction rate constant, which was reported to be 5.52 x 10^{-11} cm^3/molecule s.[41,42]

The photoionization mass spectra are measured with the krypton discharge lamp and Figure 4(a) shows a typical inverse intensity of the CH_3 signals in the mass spectra versus reaction time, obtained through adjusting the distance between the tip of the injector and

the detection region. A good linearity can be fitted between the inverse intensity of the CH_3 signals and the reaction time, providing a good illustration of the kinetics of a second-order reaction. Taking into account the available rate constant of this self-reaction,[41,42] the initial concentration of the methyl radical can be estimated from the fitted slope. Indeed, plotting $1/f[CH_3]$ instead of $1/[CH_3]$ transforms equation (8a) into

$$\frac{1}{f[CH_3]} = \frac{1}{f[CH_3]_0} + \frac{2k_1 t}{f} \qquad (8b)$$

with f being the calibration factor of the mass spectra for CH_3 radicals. From the slope we obtain f = 2.4 x 10^{-8} cm^3/molecule, which leads through extrapolation to t = 0 to $[CH_3]_0$ = (6.7 ± 1.8) x 10^{12} cm^{-3}. This value is smaller than the value expected from the F-atom concentration of 2.7 x 10^{13} cm^{-3} (obtained by supposing a 90% dissociation of $[F_2]$ = 1.5 x 10^{13} cm^{-3} in the microwave discharge), meaning that a number of F-atoms has been lost on their way to the reaction region in the long injector possibly through secondary reactions and surface reaction. Some possible schemes like replacing the discharge pyrex tube with an aluminum tube and changing the generation of F-atom from the injector to an arm of the main tube will be tested in the future to reduce the loss of F-atoms. The error bar of the initial concentration of the methyl radical includes only the statistical uncertainty of the fitted intercept, but another error source has to be taken into account: the uncertainty in the time axis, estimated to ~ 0.5 ms. Indeed, in flow tube experiments the time zero is not well defined because mixing between the gas flows from the injector and the reactor (F-atoms and CH_4 in our case) takes some time. Also, the generation of CH_3 radicals through reaction (5) takes some time, in our case (with k_5 = 6.2 x 10^{-11} cm^3/molecule s^{-1}[43] and $[CH_4]$ = 7.6 x 10^{13} cm^{-3}) 90% of F-atoms have been transformed into CH_3 radicals after ~ 0.5 ms.

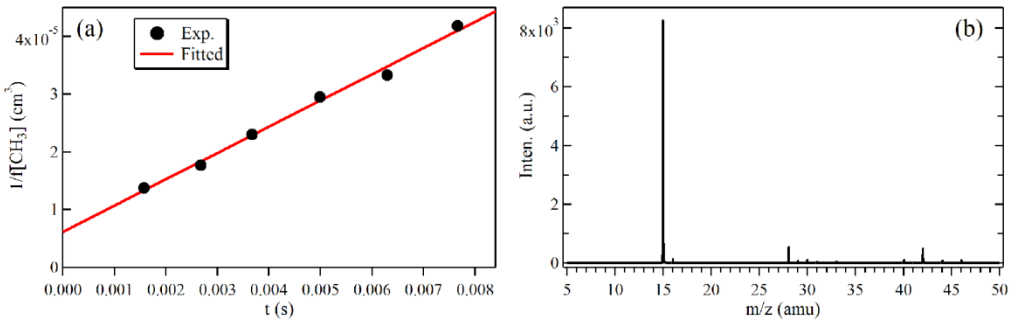

Figure 4. (a) In the self-reaction of the CH_3 radical, the inverse intensity of the CH_3 concentration

changes linearly with reaction time. (b) Photoionization mass spectrum obtained with a methyl radical concentration of ~ 1.4 x 10^{12} cm^{-3}. Both results were acquired with the krypton discharge lamp as photoionization light source.

The photoionization mass spectrum with a methyl radical concentration of ~ 1.4 x 10^{12} cm^{-3} is displayed in Figure 4(b). A very intense peak at m/z = 15 corresponding to the methyl radical can be clearly identified in the mass spectrum. For the main product ethane (m/z = 30), its IE locates at 11.52 eV,[44] above the photon energies of the krypton discharge lamp, and is not observed in the mass spectrum. Two other weak peaks at m/z = 28 and 29 are assigned to the minor products of ethylene (IE = 10.51 eV) and the ethyl radical (IE = 8.12 eV)[44], formed in secondary reactions of C_2H_6 with F-atoms. The limit of detection[40] of the methyl radical is obtained from the photoionization mass spectrum and its value is measured to be about 2 x 10^8 cm^{-3}, corresponding to a ratio of ~ 3 ppb.

3.4 The $CH_3 + O_2$ reaction

The reaction of the methyl radical, CH_3, with molecular oxygen plays a major role in the hydrocarbon oxidation and has been the focus of numerous theoretical and experimental investigations.[1,5,16] By adding oxygen to the fast flow tube, the methyl radicals, generated through above reactions (4) and (5), can react with O_2 and produce the methyl peroxy radical, CH_3O_2, via the following reaction,

$$CH_3 + O_2 + M \rightarrow CH_3O_2 + M \qquad (9)$$

where M represents any molecule removing internal energy from the nascent methyl peroxy radical in collisions. In our case, these collision partners are mostly helium, used as carrier gas, oxygen and methane.

The synchrotron-based photoionization mass matrix correlated to the $CH_3 + O_2$ reaction, shown in Figure 5(a), is recorded by scanning the synchrotron photon energy in the range of 9 - 12 eV. The matrix provides a global picture of the mass and the IEs or appearance energies (AEs) of each species involved in the reactions. In addition, the matrix can be sliced horizontally or vertically to get the photoionization mass spectra at different photon energies or the PIES corresponding to each mass.

Figure 5(b) presents the synchrotron photoionization mass spectrum at a fixed photon energy of hν = 12 eV, with 10 time magnified data in blue. Several peaks can be identified in the mass spectrum, with the two peaks at m/z = 15 and 47 being assigned to the methyl radical and the methyl peroxy radical, generated in the reactions of (5) and (9).

The peaks at m/z = 32 are from the photoionization of oxygen by the residual higher harmonic photons of the synchrotron beamline. Furthermore, some other peaks can be observed in the mass spectrum too, corresponding to the products of secondary reactions in the flow tube.

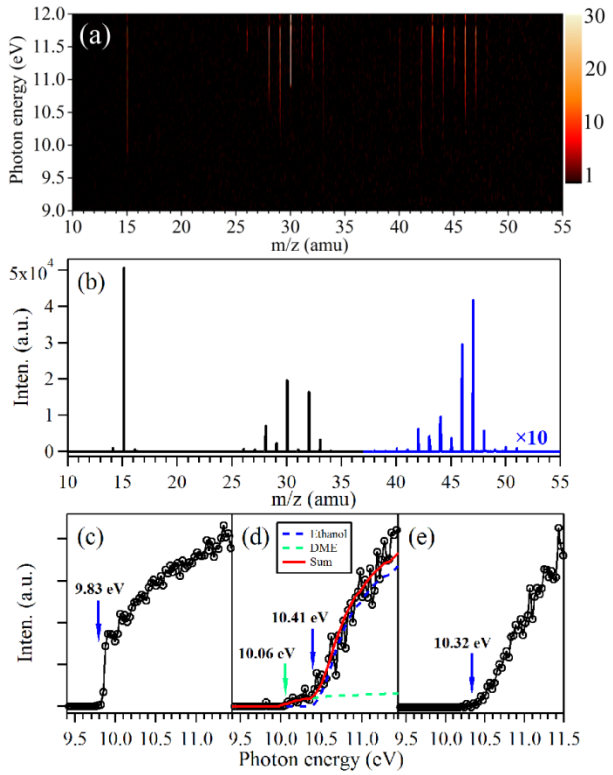

Figure 5. (a) Synchrotron-based photoionization mass matrix without the normalization of photon flux in the energy range of 9 – 12 eV, (b) the photoionization mass spectrum at hν = 12 eV, and the PIES curves corresponding to the masses of (c) m/z = 15, (d) m/z = 46 and (e) m/z = 47.

The PIES corresponding to each mass is also extracted from the matrix and their individual IEs can be obtained, which can be used to confirm the structure of the species and discriminate isomers. The PIES of m/z = 15, 46 and 47 have been chosen as examples and are shown in Figure 5(c, d, e). In the PIES of m/z = 15, the ion signal appears vertically at hν = 9.83 ± 0.03 eV, according to the adiabatic ionization energy of the methyl radical and agreeing well with the literature data.[20,45] Based on the IE of 10.32 ± 0.03 eV observed in the PIES of Figure 5(e), the species of m/z = 47 can be determined as the methyl peroxy radical.[16,46] The PIE in Figure 5(d) is fitted well with literature data[47-49] and two isomers of the m/z = 46 mass have been identified. At the beginning the ion signal appears at hν = 10.06 ± 0.03 eV and corresponds to dimethyl ether (DME,

CH_3OCH_3).[44] The ion signals can be found at hν = 10.41 ± 0.03 eV in the PIES of ethanol (C_2H_5OH) and is attributed to its IE.[44]

As we discussed in the Sec. 3.1, the present photoionization mass spectrometer has a high mass resolution and thus some isobaric species can be identified directly in the mass spectrum. Figure 6(a) shows the enlarged photoionization mass spectrum in the mass range of 28.8 – 30.2 amu recorded at the fixed synchrotron photon energy hν = 12 eV. The intense peak at m/z = 30 has two partially separated components with their centers at m/z = 30.01 and 30.05 and can be assigned as the isobaric species of formaldehyde (CH_2O) and ethane (C_2H_6), respectively. In addition, the weak peak at the isobaric mass of m/z = 29 also has two different components with their accurate mass centers at m/z = 29.00 and 29.04. The mass peak at m/z = 29.04 is attributed to the ethyl radical (C_2H_5), whose IE locates at 8.117 eV[44]. The m/z = 29.00 peak is assigned as CHO^+ and might have two origins, photoionization of the formyl radical (CHO) and dissociative photoionization of formaldehyde (CH_2O). The IE of the formyl radical locates at 8.12 eV and the AE of the CHO^+ fragment ion in dissociative photoionization of formaldehyde is at 11.97 eV.[44] Normally these two processes and their ratios can be discriminated and measured in fitting the PIE.

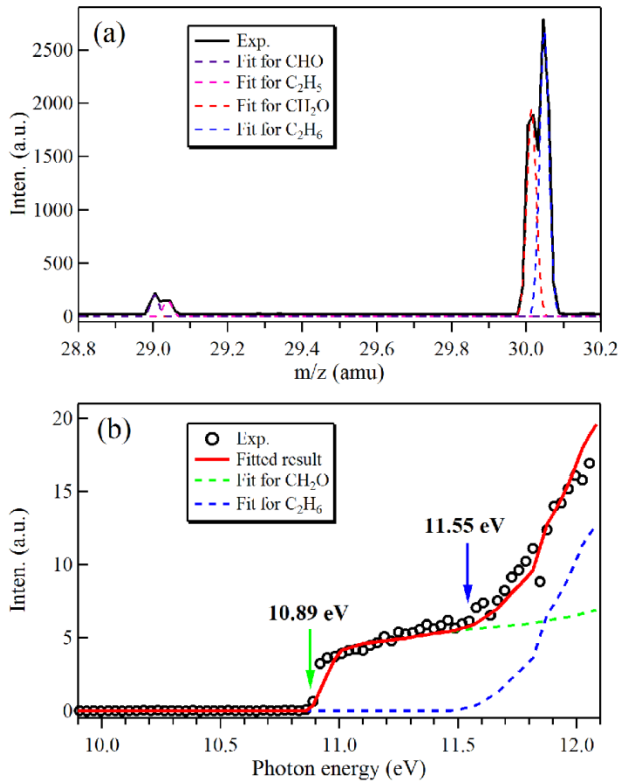

Figure 6. (a) High resolution mass spectrum recorded at fixed synchrotron photon energy hν = 12 eV, where the two isobaric peaks are assigned as CHO, C_2H_5, CH_2O and C_2H_6, respectively. (b) PIES of m/z = 30 in the energy range of 10 – 12 eV, together with the fitted results of the isobaric species formaldehyde (CH_2O) and ethane (C_2H_6).

The PIES of the isobaric mass m/z = 30 is acquired and presented in Figure 6(b). We can see that the ion signal firstly appears at hν = 10.89 ± 0.03 eV and then increases abruptly again at hν = 11.55 ± 0.03 eV, corresponding to the IEs of formaldehyde (CH_2O) and ethane (C_2H_6) and agrees well with the above high-resolution mass spectrum.[44] The ratios of each isobaric species or isomer can be determined by fitting the PIES with their absolute photoionization cross sections.[49-52] As shown in Figure 6(b), the fit of the PIES yields a ratio of 23% CH_2O and 77% C_2H_6. We have also tried to measure the ratio of the CHO^+ ion and the ethyl radical ion ($C_2H_5^+$) in the PIES of m/z = 29, but this failed, because the signal is too weak and noisy to allow a reliable fitting. Other reactants and products, together with the isomeric- or isobaric-specific species measurement, from both the primary and the secondary reactions can be efficiently determined in the photoionization mass spectra and PIES to reveal the complex reaction mechanisms involved in the fast flow tube reactor.

Now we focus on the rate constant of the reaction of methyl radical with molecular

oxygen. As listed in reaction (9), this reaction is a pressure-dependent third-order reaction and the CH_3 concentration changes with time through the relation,

$$\frac{d[CH_3]}{dt} = -k\,[CH_3][O_2][M] \qquad (10)$$

where $[O_2]$ is the concentration of oxygen and [M] is the concentration of collision molecules removing internal energy of the methyl peroxy radical. In the present experiments, the pressure of the flow tube is fixed at 2 Torr and the concentrations of O_2 and M are much higher than that of CH_3. And thus the following approximation is valid.

$$\ln[CH_3] = \ln[CH_3]_0 - k' t \qquad (11)$$

where the pseudo first-order rate constant k' = $k[O_2][M]$. The concentration of CH_3 is proportional to I_{CH3}, its ion intensity in the mass spectrum, and so we get the equation below, in which I_{CH30} is the ion intensity of CH_3 with its initial concentration.

$$\ln(I_{CH3}) = \ln(I_{CH30}) - k' t \qquad (12)$$

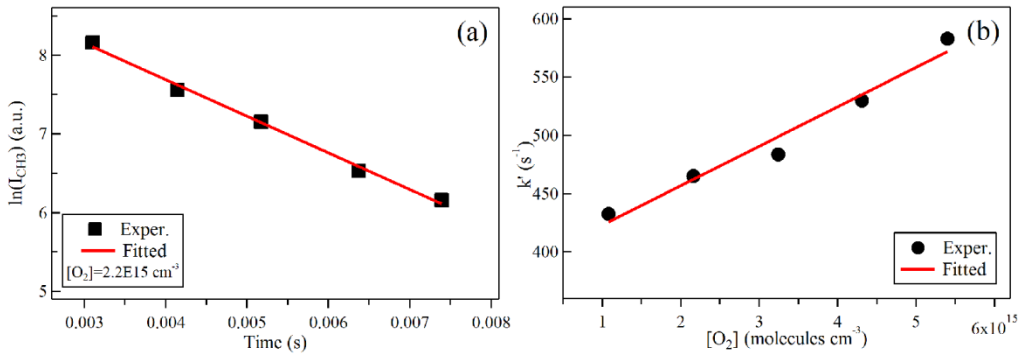

Figure 7. (a) Plot of the logarithmic ion intensity of the methyl radical in the mass spectrum versus reaction time, with the initial oxygen concentration of $[O_2] = 2.2 \times 10^{15}$ cm^{-3}. (b) Plot of the pseudofirst-order rate constant versus oxygen concentration. The pressure of the flow tube is fixed at 2 Torr.

A typical decay of the ion intensity of CH_3 versus time with the initial oxygen concentration of $[O_2] = 2.2 \times 10^{15}$ cm^{-3} is displayed in Figure 7(a) and a good linearity can be found between the logarithmic ion intensity and time, agreeing well with the hypothesis of pseudo first-order conditions. The pseudo first-order rate constant k' can be extracted from the slope of the plot of Figure 7(a) and the pseudo first-order rate constants with different oxygen concentrations are obtained and presented in Figure 7(b). The rate constant k for the reaction of the methyl radical with oxygen at 2 Torr and 298 K is obtained as the slope of Figure 7(b) and found to be $(4.9 \pm 1.4) \times 10^{-31}$ $cm^6 molecule^{-2} s^{-1}$, in agreement well with the existing literature data[53,54].

4. Conclusions

A highly sensitive VUV photoionization orthogonal TOF mass spectrometer combined with a microwave discharge generator and a fast flow tube reactor has been constructed for the study of gas-phase radical reactions. The reactions are initiated by fluorine atoms produced in a microwave discharge and the reaction time is changed through adjusting the distance between the tip of the injector and the detection region. Two kinds of VUV photoionization light sources, the continuously tunable VUV synchrotron radiation at Hefei and a commercial krypton discharge lamp have been used for isomer-specific product detection and time-consuming kinetic measurements respectively in the apparatus. The combination of the continuous photoionization light sources and the continuous molecular beam sampling is beneficial to maximize the species detection. The performances of the setup including the mass resolution ($M/\Delta M$ ~ 2100, FWHM) and the limit of detection (LOD ~ 0.8 ppb) have been tested and are presented here.

The self-reaction of the methyl radical and the reaction of the methyl radical with molecular oxygen have been chosen as benchmarks to evaluate the system. The self-reaction of the methyl radical provides a good illustration of the kinetics of a second-order reaction. Multiple species including radicals and intermediates from both primary and secondary reactions are simultaneously detected in the photoionization mass spectra. The isomeric and isobaric products are successfully identified and their mole fractions are measured in the photoionization efficiency spectra by scanning the synchrotron photon energy. These preliminary results have demonstrated the multiplex capabilities of the present apparatus of the VUV photoionization mass spectrometer/fast flow tube, even with a commercial discharge lamp. The present experimental system will provide new valuable insights into radical reactions, especially of atmospheric and combustion interests. Furthermore, another microwave discharge generator will be added on the fast flow tube reactor in the imminent future and then kinetics and reaction mechanisms of radical-radical reactions can also be investigated.

Acknowledgments

This work was supported by the National Key Research and Development Program of China (2016YFC0200300), the National Natural Science Foundation of China

(21773249, 91644109), the International Partnership Program of Chinese Academy of Sciences (116134KYSB20170048) and the Natural Science Foundation of Anhui Province (1608085MB35). The authors thank Dr. Zhongyue Zhou (Shanghai Jiao Tong University, China) for helpful discussion in designing the photoionization mass spectrometer. C.F. would like to thank funding support of Chinese Academy of Sciences President's International Fellowship Initiative (2018VMA0055). The authors are also grateful to the NSRL staffs for smoothly running the synchrotron facility and providing beamtime.

References

1. Orlando JJ, Tyndall GS. Laboratory studies of organic peroxy radical chemistry: an overview with emphasis on recent issues of atmospheric significance. *Chem. Soc. Rev.* 2012; 41: 6294-6317.

2. Savee JD, Papajak E, Rotavera B, Huang H, Eskola AJ, Welz O, Sheps L, Taatjes CA, Zador J, Osborn DL. Direct observation and kinetics of a hydroperoxyalkyl radical (QOOH). *Science* 2015; 347: 643-646.

3. Qi F. Combustion chemistry probed by synchrotron VUV photoionization mass spectrometry. *P. Combust. Inst.* 2013; 34: 33-63.

4. Osborn DL. Reaction mechanisms on multiwell potential energy surfaces in combustion (and atmospheric) chemistry. *Annu. Rev. Phys. Chem.* 2017; 68: 233-260.

5. Tyndall G, Cox R, Granier C, Lesclaux R, Moortgat G, Pilling M, Ravishankara A, Wallington T. Atmospheric chemistry of small organic peroxy radicals. *J. Geophys. Res-Atmos.* 2001; 106: 12157-12182.

6. Mollner AK, Valluvadasan S, Feng L, Sprague MK, Okumura M, Milligan DB, Bloss WJ, Sander SP, Martien PT, Harley RA. Rate of gas phase association of hydroxyl radical and nitrogen dioxide. *Science* 2010; 330: 646-649.

7. Sprague MK, Mertens LA, Widgren HN, Okumura M, Sander SP, McCoy AB. Cavity ringdown spectroscopy of the hydroxy-methyl-peroxy radical. *J. Phys. Chem. A* 2013; 117: 10006-10017.

8. Assaf E, Sheps L, Whalley L, Heard D, Tomas A, Schoemaecker C, Fittschen C. The reaction between CH_3O_2 and OH radicals: Product yields and atmospheric implications. *Environ. Sci. Technol.* 2017; 51: 2170-2177.

9. Noziere B, Hanson DR. Speciated monitoring of gas-phase organic peroxy radicals by chemical ionization mass spectrometry: Cross-reactions between CH_3O_2, $CH_3(CO)O_2$, $(CH_3)_3CO_2$, and c-$C_6H_{11}O$. *J. Phys. Chem. A* 2017; 121: 8453-8464.

10. Berndt T, Scholz W, Mentler B, Fischer L, Herrmann H, Kulmala M, Hansel A. Accretion product formation from self- and cross-reactions of RO_2 radicals in the atmosphere. *Angew. Chem. Int. Ed.* 2018; 57: 3820-3824.

11. Slagle IR, Gutman D. Kinetics of polyatomic free-radicals produced by laser photolysis. 5. Study of the equilibrium $CH_3 + O_2$ reversible CH_3O_2 between 421 and 538 degrees. *J. Am. Chem. Soc.* 1985; 107: 5342-5347.

12. Loison J-C, Sanglar S, Villenave E. Discharge flow tube coupled to time-of-

flight mass spectrometry detection for kinetic measurements of interstellar and atmospheric interests. *Rev. Sci. Instrum.* 2005; 76: 053105.

13. Osborn DL, Zou P, Johnsen H, Hayden CC, Taatjes CA, Knyazev VD, North SW, Peterka DS, Ahmed M, Leone SR. The multiplexed chemical kinetic photoionization mass spectrometer: A new approach to isomer-resolved chemical kinetics. *Rev. Sci. Instrum.* 2008; 79: 104103.

14. Howard CJ. Kinetic measurements using flow tubes. *J. Phys. Chem.* 1979; 83: 3-9.

15. Kaufman F. Kinetics of elementary radical reactions in the gas phase. *J. Phys. Chem.* 1984; 88: 4909-4917.

16. Meloni G, Zou P, Klippenstein SJ, Ahmed M, Leone SR, Taatjes CA, Osborn DL. Energy-resolved photoionization of alkylperoxy radicals and the stability of their cations. *J. Am. Chem. Soc.* 2006; 128: 13559-13567.

17. Qi F, Yang R, Yang B, Huang C, Wei L, Wang J, Sheng L, Zhang Y. Isomeric identification of polycyclic aromatic hydrocarbons formed in combustion with tunable vacuum ultraviolet photoionization. *Rev. Sci. Instrum.* 2006; 77: 084101.

18. Pan Y, Hu Y, Wang J, Ye L, Liu C, Zhu Z. Online characterization of isomeric/isobaric components in the gas phase of mainstream cigarette smoke by tunable synchrotron radiation vacuum ultraviolet photoionization time-of-flight mass spectrometry and photoionization efficiency curve simulation. *Anal. Chem.* 2013; 85: 11993-12001.

19. Cool TA, Nakajima K, Mostefaoui TA, Qi F, McIlroy A, Westmoreland PR, Law ME, Poisson L, Peterka DS, Ahmed M. Selective detection of isomers with photoionization mass spectrometry for studies of hydrocarbon flame chemistry. *J. Chem. Phys.* 2003; 119: 8356-8365.

20. Zhu Y, Wu X, Tang X, Wen Z, Liu F, Zhou X, Zhang W. Synchrotron threshold photoelectron photoion coincidence spectroscopy of radicals produced in a pyrolysis source: The methyl radical. *Chem. Phys. Lett.* 2016; 664: 237-241.

21. Tang X, Lin X, Zhu Y, Wu X, Wen Z, Zhang L, Liu F, Gu X, Zhang W. Pyrolysis of n-butane investigated using synchrotron threshold photoelectron photoion coincidence spectroscopy. *RSC Advances* 2017; 7: 28746-28753.

22. Garcia GA, Tang X, Gil J-F, Nahon L, Ward M, Batut S, Fittschen C, Taatjes CA, Osborn DL, Loison J-C. Synchrotron-based double imaging photoelectron/photoion coincidence spectroscopy of radicals produced in a flow tube: OH and OD. *J. Chem. Phys.* 2015; 142: 164201.

23. Sztáray B, Voronova K, Torma KG, Covert KJ, Bodi A, Hemberger P, Gerber T, Osborn DL. CRF-PEPICO: Double velocity map imaging photoelectron photoion coincidence spectroscopy for reaction kinetics studies. *J. Chem. Phys.* 2017; 147: 013944.

24. Bodi A, Hemberger P, Osborn DL, Sztáray B. Mass-resolved isomer-selective chemical analysis with imaging photoelectron photoion coincidence spectroscopy. *J. Phys. Chem. Lett.* 2013; 4: 2948-2952.

25. Krüger J, Garcia GA, Felsmann D, Moshammer K, Lackner A, Brockhinke A, Nahon L, Kohse-Höinghaus K. Photoelectron–photoion coincidence spectroscopy for multiplexed detection of intermediate species in a flame. *Phys. Chem. Chem. Phys.* 2014; 16: 22791-22804.

26. Zhou Z, Wang Y, Tang X, Wu W, Qi F. A new apparatus for study of pressure-

dependent laminar premixed flames with vacuum ultraviolet photoionization mass spectrometry. *Rev. Sci. Instrum.* 2013; 84: 014101.

27. Zhou Z, Du X, Yang J, Wang Y, Li C, Wei S, Du L, Li Y, Qi F, Wang Q. The vacuum ultraviolet beamline/endstations at NSRL dedicated to combustion research. *J. Synchrotron Rad.* 2016; 23: 1035-1045.

28. Tang X, Zhou XG, Niu ML, Liu SL, Sun JD, Shan XB, Liu FY, Sheng LS. A threshold photoelectron-photoion coincidence spectrometer with double velocity imaging using synchrotron radiation. *Rev. Sci. Instrum.* 2009; 80: 113101.

29. Bodi A, Hemberger P, Gerber T, Sztaray B. A new double imaging velocity focusing coincidence experiment: i^2PEPICO. *Rev. Sci. Instrum.* 2012; 83: 083105.

30. Garcia G, Cunha de Miranda B, Tia M, Daly S, Nahon L. DELICIOUS III: A multipurpose double imaging particle coincidence spectrometer for gas phase vacuum ultraviolet photodynamics studies. *Rev. Sci. Instrum.* 2013; 84: 053112.

31. Tang X, Garcia GA, Gil J-F, Nahon L. Vacuum upgrade and enhanced performances of the double imaging electron/ion coincidence end-station at the vacuum ultraviolet beamline DESIRS. *Rev. Sci. Instrum.* 2015; 86: 123108.

32. Falkovich G, *Fluid Mechanics*; Cambridge University Press: 2011.

33. Guilhaus M, Selby D, Mlynski V. Orthogonal acceleration time-of-flight mass spectrometry. *Mass Spectrom. Rev.* 2000; 19: 65-107.

34. Hall RI, McConkey A, Ellis K, Dawber G, Avaldi L, Macdonald MA, King GC. A penetrating field electron-ion coincidence spectrometer for use in photoionization studies. *Meas. Sci. Technol.* 1992; 3: 316-324.

35. Adams A, Read FH. Electrostatic cylinder lenses II: Three element einzel lenses. *J. Phys. E: Sci. Instrum.* 1972; 5: 150-155.

36. Nemeth GI, Selzle HL, Schlag EW. Magnetic ZEKE experiments with mass analysis. *Chem. Phys. Lett.* 1993; 215: 151-155.

37. Lu KT, Eiden GC, Weisshaar JC. Toluene cation: Nearly free rotation of the methyl group. *J. Phys. Chem.* 1992; 96: 9742-9748.

38. Bralsford R, Harris PV, Price WC. The effect of fluorine on the electronic spectra and ionization potential molecules. *Proc. R. Soc. Lond. A* 1960; 258: 459-469.

39. Williams BA, Tanada TN, Cool TA, In *Twenty-Fourth Symposium (International) on Combustion*, The Combustion Institute: Pittsburgh, PA, 1992; pp 1587-1596.

40. Heger HJ, Zimmermann R, Dorfner R, Beckmann M, Griebel H, Kettrup A, Boesl U. On-line emission analysis of polycyclic aromatic hydrocarbons down to pptv concentration levels in the flue gas of an incineration pilot plant with a mobile resonance enhanced multiphoton ionization time-of-flight mass spectrometer. *Anal. Chem.* 1999; 71: 46-57.

41. Wang BS, Hou H, Yoder LM, Muckerman JT, Fockenberg C. Experimental and theoretical investigations on the methyl-methyl recombination reaction. *J. Phys. Chem. A* 2003; 107: 11414-11426.

42. Riffault V, Bedjanian Y, Le Bras G. Kinetics and mechanism of the O atom reaction with dimethyl sulfoxide. *J. Phys. Chem. A* 2003; 107: 5404-5411.

43. Persky A. Kinetics of the reactions F+H_2S and F+D_2S at 298 K. *Chem. Phys. Lett.* 1998; 298: 390-394.

44. NIST Chemistry WebBook. In http://webbook.nist.gov/chemistry/ (retrieved 1 October, 2018).

45. Schulenburg AM, Alcaraz C, Grassi G, Merkt F. Rovibrational photoionization dynamics of methyl and its isotopomers studied by high-resolution photoionization and photoelectron spectroscopy. *J. Chem. Phys.* 2006; 125: 104310.

46. Voronova K, Ervin KM, Torma KG, Hemberger P, Bodi A, Gerber T, Osborn DL, Sztaray B. Radical thermometers, thermochemistry, and photoelectron spectra: a PEPICO study of the methyl peroxy radical. *J. Phys. Chem. Lett.* 2018; 9: 534-539.

47. Person JC, Nicole PP. Isotope effects in photoionization yields and in absorption cross sections for methanol, ethanol, methyl bromide, and ethyl bromide. *J. Chem. Phys.* 1971; 55: 3390-3397.

48. Koizumi H. Predominant decay channel for superexcited organic molecules. *J. Chem. Phys.* 1991; 95: 5846-5852.

49. Photonionization Cross Section Database. In http://flame.nsrl.ustc.edu.cn/database/data.php (retrieved 1 October, 2018).

50. Cool TA, Wang J, Nakajima K, Taatjes CA, McIlroy A. Photoionization cross sections for reaction intermediates in hydrocarbon combustion. *Int. J. Mass spectrom.* 2005; 247: 18-27.

51. Wang J, Yang B, Cool TA, Hansen N, Kasper T. Near-threshold absolute photoionization cross-sections of some reaction intermediates in combustion. *Int. J. Mass spectrom.* 2008; 269: 210-220.

52. Cooper G, Anderson JE, Brion CE. Absolute photoabsorption and photoionization of formaldehyde in the VUV and soft X-ray regions (3-200 eV). *Chem. Phys.* 1996; 209: 61-77.

53. Pilling MJ, Smith MJC. A laser flash photolysis study of the reaction CH_3+O_2 --> CH_3O_2 at 298 K. *J. Phys. Chem.* 1985; 89: 4713-4720.

54. Pratt GL, Wood SW. Kinetics of the reaction of methyl radicals with oxygen. *J. Chem. Soc., Faraday Trans. 1* 1984; 80: 3419-3427.